Preprint: Submitted - before peer review

No going back - Limited reversibility of regional climate changes under overshoot

Peter Pfleiderer (1,2), Carl-Friedrich Schleussner (2,3), Jana Sillmann (1,4)

1 Universität Hamburg, Germany
2 Climate Analytics, Germany
3 Humboldt Universität, Berlin, Germany
4 CICERO - Center for International Climate Research Oslo, Norway

E-mail: peter.pfleiderer@climateanalytics.org

Arpil 2023

Abstract.

Without stringent reductions in emission of greenhouse gases in the coming years, an exceedance of the 1.5C temperature limit would become increasingly likely. This has given rise to so-called temperature overshoot scenarios, in which the global mean surface air temperature increase above pre-industrial levels exceeds a certain limit, i.e. 1.5C, before bringing temperatures back below that level. Despite their prominence in the climate mitigation literature, the implications of an overshoot for local climate impacts is still understudied. Here we present a comprehensive analysis of implications of an overshoot for regional temperature and precipitation changes as well as climate extremes indices. Based on a multi-model comparison from the Coupled Model Intercomparison Project (CMIP6) we find that temperature changes are largely reversible in most regions, but also report significant land-ocean and latitudinal differences after an overshoot. For precipitation, the emergent picture is less clear. For regions where significant changes in precipitation can be identified, a reversibility of those changes is the exception, with most regions experiencing increased drying or wetting after an overshoot. This effect is even more pronounced for extreme precipitation. Taken together, our results indicate that even under a reversal of global mean temperature increase, regional climate changes may only be partially reversible, if at all. We thus provide further evidence that overshooting of a warming level implies irreversible changes.

1. Introduction

The global mean surface air temperature increase above pre-industrial levels is about 1.3°C to date [1]. Without stringent emission reductions in the near-term, an exceedance

of 1.5°C of global warming thus becomes increasingly likely [2]. As a consequence, so-called overshoot scenarios that temporarily exceed 1.5°C before bringing temperatures back down below that level by means of net negative CO2 emissions have risen to prominence in the mitigation literature[2, 3]. For time-lagged climate impacts such as cryospheric changes or sea-level rise, temperature overshoot will lead irreversible impacts [4, 5]. However, the question of reversibility is less established for changes in atmospheric variables such as temperature and precipitation.

In observations the climate is warming globally with diverse physical impacts regionally [6] and most climate simulations are run for emission scenarios where this warming is continued. Although one would expect that regional changes reverse when climate is cooling in an overshoot scenario, there are different effects that would lead to non-linearities in the evolution of regional climate signals. While changes in some indicators such as GMST [7] or Arctic sea-ice can be reversed [8], a hysteresis is expected for parts of the carbon cycle, ocean heat content or the inter-tropical convergence zone [8, 9, 10].

One factor leading to this hysteresis is the lagged response of the ocean to increased greenhouse gas concentrations in the atmosphere. While the atmosphere responds fast to changes in greenhouse gas concentrations, the ocean has a larger inertia leading to a slower response and considerable lagged effects that will still change the climate for decades and centuries [11, 12, 13, 14]. This already implies that the transient state of a 1.5C climate is different from a climate state that is stabilized at 1.5C [15, 16]. The period after peak warming in an overshoot scenario is an extreme case where the instantaneous effect of CO2 reduction is superimposed by the lagged effect of CO2 increases of the decades before peak warming.

Besides the superposition of a fast response to decreasing CO2 concentrations and a slow response to the warming of the decades before peak warming, local feedback mechanisms as well as changes in aerosol concentrations can contribute to differences in climate impacts between the period when the climate is still warming and the period after peak warming.

Here we present an overview of regional climate signals in two overshoot scenarios (SSP5-34-OS and SSP1-19) with a focus on regional climate signals that change their dependence on GMST throughout the overshoot. We analyze how regional climate signals evolve in the period before and after peak warming. By comparing the strength of the dependence of these changes on GMST before and after peak warming we assess to which extend changes during the warming period of the overshoot are reversed during the cooling period after peak warming. This analysis gives a first overview of climate impacts of overshooting a global warming goal and helps to identify hot-spot regions where considerable additional climate impacts have to be expected.

2. Data & Methods

2.1. Climate projections of overshoot scenarios

We analyze Earth System model simulations from the sixth phase of the Coupled Model Intercomparison Project (CMIP6 [17]) for the emission scenarios SSP5-34-OS and SSP1-19 from the Scenario Model Intercomparison Project (ScenarioMIP [18]). The SSP5-34-OS scenario is an idealized and rather unrealistic scenario where greenhouse gases are emitted at a high rate until 2040 with strong mitigation thereafter until net-zero CO2 emissions are reached in 2065 and CO2 concentrations in the atmosphere are further reduced from there on (see fig. 1a). The SSP1-19 is a strong mitigation scenario with only a moderate overshoot. In addition to these two overshoot scenarios we also use pre-industrial control simulations (piControl) to compare regional trends in the overshoot scenarios to trends originating from internal climate variability.

We aggregate the gridded climate projections into 46 land regions and 12 oceanic regions (see fig. 12) following the regional aggregation of the sixth assessment report of the Intergovernmental Panel on Climate Change [6]. For land regions, we only consider grid-cells that are considered as land-cells in the model and vise versa for ocean regions. When averaging over grid-cells of one regions, grid-cells are weighted by their area within the region.

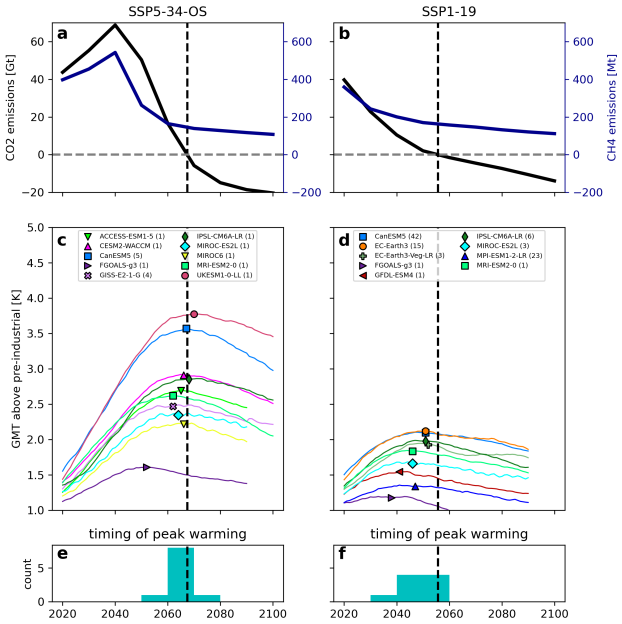

Figure 1. a: CO2 emissions (left y-axis) and methane emissions (right y-axis) since 2020 in the SSP5-34-OS scenario. c: Global mean surface temperature (GMST) projections from CMIP6 for the SSP5-34-OS scenario. e: timing of peak warming in the CMIP6 projections of the SSP5-34-OS scenario. b: as (a) but for the SSP1-19 scenario. d: as (c) but for the SSP1-19 scenario. f: as (e) but for the SSP1-19 scenario.

For our analysis, we exclude runs that do not cool down to 0.2K below peak warming

Table 1. Number of analyzed simulation runs grouped by CMIP6 model and scenario. The number of available runs with monthly or daily output differs and is provided separately.

	monthly		daily	
Model name	SSP5-34-OS	SSP1-19	SSP5-34-OS	SSP1-19
ACCESS-ESM1-5	1			
CESM2-WACCM	1			
CanESM5	5	42		42
EC-Earth3		15		14
EC-Earth3-Veg-LR		3		3
FGOALS-g3	1	1		
GFDL-ESM4		1		1
GISS-E2-1-G	4			
IPSL-CM6A-LR	1	6		6
MIROC-ES2L	1	3	1	3
MIROC6	1			
MPI-ESM1-2-LR		23		23
MRI-ESM2-0	1	1		1
UKESM1-0-LL	1			

until 2100 (for 31-year averaged GMST). The used models as well as the number of runs for each of the scenarios is listed in table 1.

Besides monthly surface air temperature (tas) and precipitation (pr), three climate extreme indices are analyzed: The yearly maximum of daily maximum temperatures (TXx), the yearly minimum of daily minimum temperatures (TNn) and the yearly maximum daily precipitation (RX1day). These indices were calculated for runs for which daily maximum air temperature, daily minimum air temperature and daily precipitation is available (see table 1).

2.2. Peak warming

GMST trajectories are smoothed with a 31-year running average. The timing of *peak warming* in each simulation is defined as the average of all years in which the smoothed GMST is less than 0.025K smaller than the highest GMST value in the simulation.

$$peak\ timing = \overline{\{year \mid GMST_{max} - GMST(year) < 0.025K\}} \tag{1}$$

As shown in figure 1, global mean surface temperatures peak around the time when net-zero CO_2 emissions are reached. In the SSP5-34-OS scenario most models reach peak warming between 2060 and 2070. In the SSP1-19 scenario, most ESMs reach their peak GMST between 2040 and 2060.

2.3. Period before and after peak warming

In the following, changes in regional climate signals before and after peak warming are analyzed. To allow comparability, the periods before and after peak warming have the same length (30-40 years depending on timing of peak warming). This period length is limited by period between peak warming and the end of the simulations. For each simulation run this period length is assessed individually. We do not consider simulations after 2100 as they are only available for a very small set of models.

2.4. Dependence of regional climate variables on GMST

In each simulation we compare the strength of the dependence of regional climate signals on GMST before and after peak warming. As an estimate of the dependence on GMST we use the slope β of a linear regression between the climate signal and GMST. If the median of the trends from simulation runs of a model after peak warming is 50% stronger than before or vice versa we consider the dependence on GMST as different. Note that for many models only one simulation is available and this change in GMST dependence should be interpreted with caution.

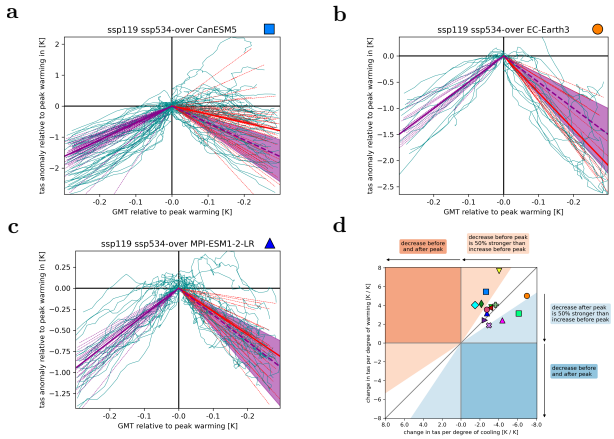

Figure 2. Anomalies in annual mean surface air temperature over the Arctic Ocean (turquoise lines) plotted against an unconventional x-axis: GMST anomalies with respect to peak warming GMST until peak warming (vertical dashed line) and the same from there on but after peak warming. The purple and red lines indicate the trends versus GMST before and after peak warming. The trend lines are shifted such that they all meet at peak warming. The thicker lines indicate the ensemble median trends. For the period after peak warming, the median trend from before peak warming is shown as a thick dashed purple line. The shading around this line indicates the area in which the trend after peak warming would not differ by a factor of 1.5. a: CanESM5 simulations. b: GISS-E2-1-G simulations. c: MPI-ESM1-2-LR simulations. d: Overview scatter plot showing change in tas per degree of GMST warming before peak warming versus change in tas per degree of GMST cooling after peak warming. The upper left and bottom right quadrants are colored in dark red and dark blue to indicate locations where tas changes are continued after peak warming. The light shading in the upper right and bottom left quadrants indicate the regions where the dependence on GMST after peak is considerably differs from the dependence on GMST before peak warming based on the analysis explained in section 2.4.

2.5. Detection of robust changes

The main analysis is based on forced changes in local climate signals before and after peak warming. Evaluating whether a simulated trend has been forced by changes in GMST is challenging as the changes in GMST around peak warming are relatively slow (particularly in SSP1-19) and the analyzed periods can be quite short. The simulated trends in regional climate signals can be in the range of trends that could occur as a result of internal climate variability. Therefore, for each period (before and after peak warming) we test whether the trend is common in control simulations without anthropogenic forcing (piControl). If the detected trend exceeds the 95th (or is below the 5th) percentile of all trends found over periods of identical length in piControl simulations we reject the null-hypothesis that the detected trend is a result of internal climate variability.

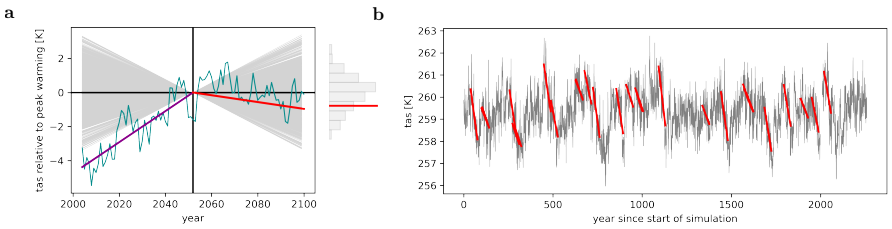

Figure 3. a: Annual mean surface air temperature over the Arctic Ocean projected for the SSP1-19 scenario by the model IPSL-CM6A-LR (turquoise). The trends before peak warming (purple) and after peak warming (red) are adjusted to match the annual temperatures in the 30-year period around peak warming. Gray lines show trends found in the piControl run that have the same length as the period before and after peak warming. These lines are also shifted with the 30-year average tas around peak warming. b: piControl simulations of annual mean temperatures for the same region. Red lines indicate periods that have stronger trends than the trend after peak warming.

The above described method is applied for models for which less than four simulations are available. If four or more simulations are available we consider changes as forced if 75% of the simulations agree on the sign of change.

2.6. Classification of behavior around peak warming

The behavior of local climate signals around peak warming is complex and requires some tedious and in-depth analysis. Here we start, by classifying the behavior around peak warming in the following flavors: "continued", "reversed", "partially reversed", "overcompensated", "stabilized", "unexpected change" and "unclear".

Table 2. Classification of evolution of local climate signals around peak warming into representative types. Combining the dependence of the local climate signal on GMST before β_{before} and after β_{after} peak warming (from sec. 2.4) with the evaluation of whether the projected trends could occur as a result of natural variability (from sec. 2.5) the evolution of the climate signal is classified in the following types: continued, reversed, partially reversed, overcompensated, stabilized, unexpected change and unclear.

sec. 2.4						sec. 2.5			
$\beta_{before} > 0$	$\beta_{before} < 0$	$\beta_{after} > 0$	$\beta_{after} < 0$	$\lvert\beta_{after}\rvert \geq 1.5 \cdot \lvert\beta_{before}\rvert$	$\lvert\beta_{before}\rvert \geq 1.5 \cdot \lvert\beta_{after}\rvert$	Robust before	Robust after		
✓		✓				✓	✓	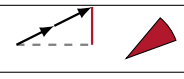	continued
	✓		✓			✓	✓	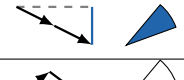	
✓			✓			✓	✓	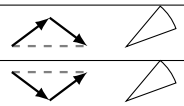	reversed
	✓	✓				✓	✓	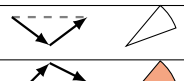	
✓			✓	✓		✓	✓	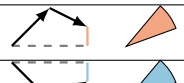	partially reversed
	✓	✓		✓		✓	✓	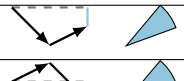	
✓			✓		✓	✓	✓		overcompensated
	✓	✓			✓	✓	✓	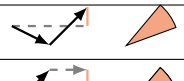	
✓						✓			stabilized
	✓					✓		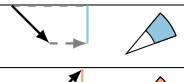	
		✓					✓	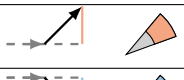	unexpected change
		✓					✓		
									unclear

For the cases *continued*, *reversed*, *partially reversed* and *overcompensated* the trends before and after peak warming have been identified as forced trends. For *reversed* the

dependence of the climate variable on GMST does not change considerably. In *partially reversed* the trend after peak warming is at least 50% less strong than before and in the case *overcompensated* the trend after peak warming is at least 50% stronger than before. In the case *continued* the dependence on GMST changes sign and the trend in the regional climate variable is continued irrespective of the change in GMST trend.

The case *stabilized* is an unexpected stabilization that can be seen as a more extreme version of *partially reversed*: while for the period before peak warming the changes in the local climate signal clearly exceed changes that could be expected from internal climate variability this is not the case after peak warming.

The case *unexpected change* is the inverse of case *stabilized* where changes cannot be differentiated from natural variability before peak warming but after peak warming a robust forced change is simulated. This case could hint towards mechanisms in the climate system that factor each other out before peak warming but do not afterwards.

Table 2 lists all the possible behaviors for temperature indicators. The color coding on the right side indicates which behaviors would lead to higher or lower temperatures at the same GMST level before and after peak warming. The color coding on the right color is used in the following to specify the behavior in an ESM.

3. Results

3.1. Surface air temperature

While greenhouse gas concentrations rise, annual mean temperature rises around the globe. Therefore, in all regions annual mean temperature increases until peak warming. When GMST is decreasing after peak warming, annual temperature also decreases and in many regions changes are reversed in the decades after peak warming (see figure 4).

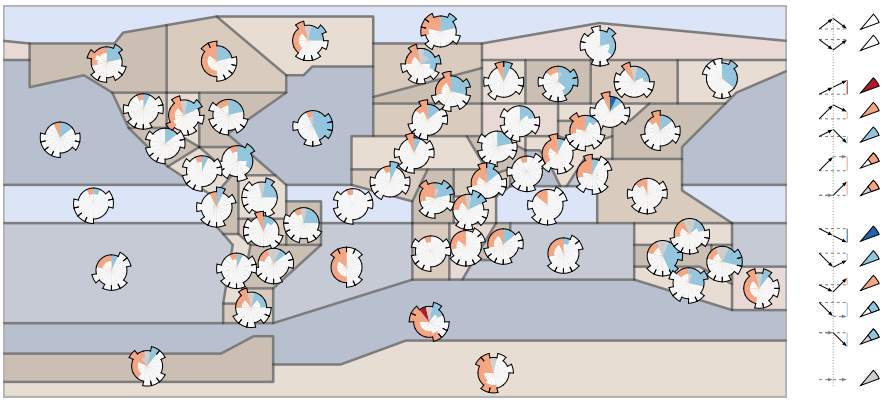

Figure 4. Changes in annual mean surface air temperature around peak warming. Each regional pie-plot follows the logic of table 2. Red (blue) colors indicate that the overshoot leads to warmer (cooler) local conditions. If the inner part of a circle segment is white (gray) it means that there is no robust trend after (before) peak warming. Large circle segments indicate that at least four runs could be analyzed for this earth system model. See figure 12 for region names.

Over the Southern Ocean (SOO) and south Atlantic (SAO) most models project a weaker cooling in the period after peak warming as compared to the warming before peak warming. As a result, at the same GMST level, annual air temperatures over these regions are projected to be warmer after peak warming than before. These findings are in line with [12] who showed that in the fast response to increases in CO2 concentrations the warming over the Southern Ocean is suppressed while in the slow response it is not. Similarly, over north eastern North America (NEN), Greenland (GIC) and the Arctic ocean (ARO) the cooling as a response to a decrease in CO2 concentrations is superimposed by a lagged warming effect from the preceeding decades.

There are also regions where models project an overall "cooling effect" of the overshoot. These regions are mostly land regions and the north Atlantic (NAO). Here, the warming before peak warming is overcompensated after peak warming leading to cooler temperatures at the same GMST level. Surface air temperatures over land regions react quickly to changes in CO2 concentrations and lagged effects only occur indirectly. Note that the relatively quicker decrease in regional temperatures could be an artifact of our method that is focused on GMST levels: while in some regions the cooling in the period after peak warming is damped by lagged warming effects (SOO) other regions have to level that effect off by cooling faster with respect to GMST.

As shown in figure 5 there are models that show a consistent hemispheric dipole pattern with warmer temperatures in the southern hemisphere after peak warming and cooler temperatures in the northern hemisphere (CESM-WACCM, GISS-E2-1-G, MRI-ESM2-0). There are, however, also models that show a consistent warming of the Arctic with diverse changes elsewhere (CanESM5, EC-Earth3-Veg-LR, FGOALS-g3). Differences in ocean dynamics between models, potentially linked to time-lagged dynamics of the Atlantic meridional overturning circulation (AMOC) [19], might be the main reason for these opposite signals in the Arctic.

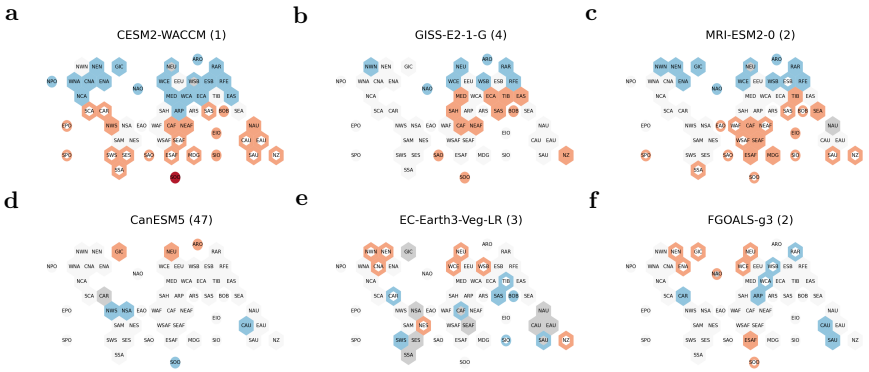

Figure 5. Changes in annual surface air temperature around peak warming. The coloring of land-region hexagons and ocean-region circles follows the logic of table 2. Red (blue) colors indicate that the overshoot leads to warmer (cooler) local conditions. If the inner part of a region is white (gray) it means that there is no robust trend after (before) peak warming.

A closer look at north east North America reveals that some of the effects of an overshoot can be quite significant, in particular on seasonal scales. When GMST has cooled down by 0.2K relative to peak warming, winter temperatures are projected to be up to 0.4K warmer or cooler as compared to the same GMST level before peak warming (see fig. 6). For spring, GFDL-ESM4 and MIROC6 project a continued warming after peak warming although the warming in the period after peak warming cannot be distinguished from natural variability. In JJA and SON there is no agreement between models and many models show a reversal of changes that are projected to occur throughout the overshoot.

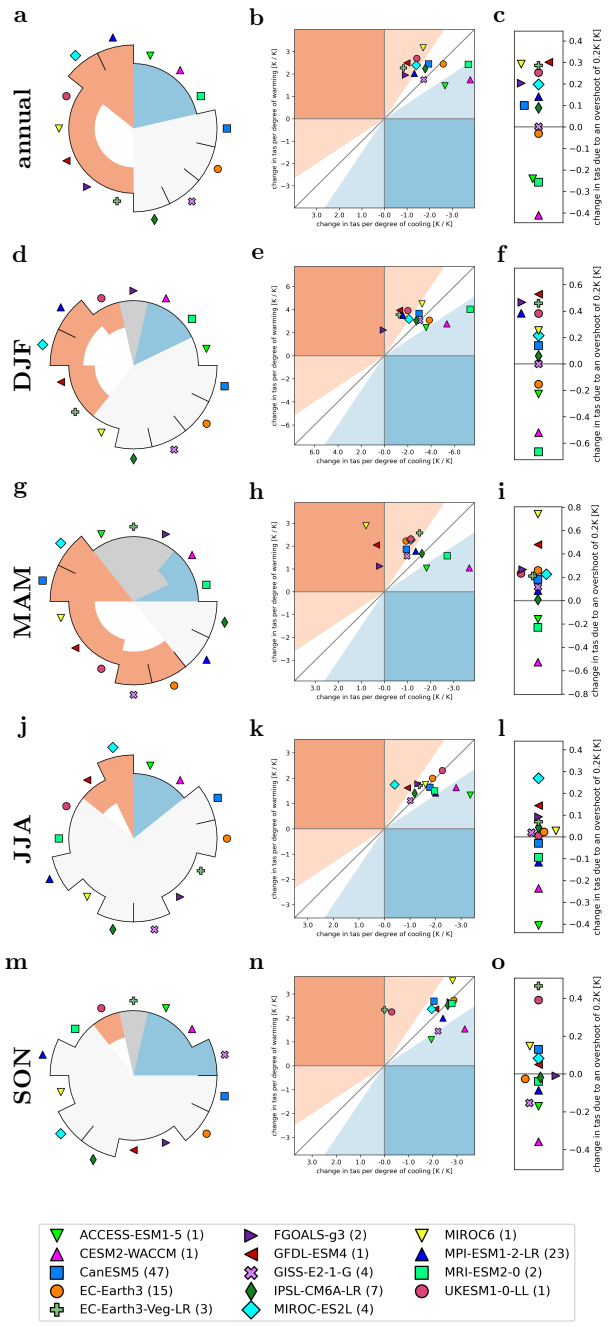

Figure 6. Changes in northeast North America annual surface air temperature around peak warming. a: pie-plots as in fig. 4. b: overview scatter plot showing change in tas per degree of GMST warming before peak warming versus change in tas per degree of GMST cooling after peak warming. The upper left and bottom right quadrants are colored in dark red and dark blue to indicate locations where tas changes are continued after peak warming. The light shading in the upper right and bottom left quadrants indicate the regions where the dependence on GMST after peak is considerably differs from the dependence on GMST before peak warming based on the analysis explained in section 2.4. c: Difference in tas between after and before peak warming at GMST levels 0.2K cooler than peak warming. These values are estimated from the trend versus GMST before and after peak warming. d-f as a-c but for December-February. g-i as a-c but for March-Mai. j-l as a-c but for June-August. m-o as a-c but for September-November.

3.2. Precipitation

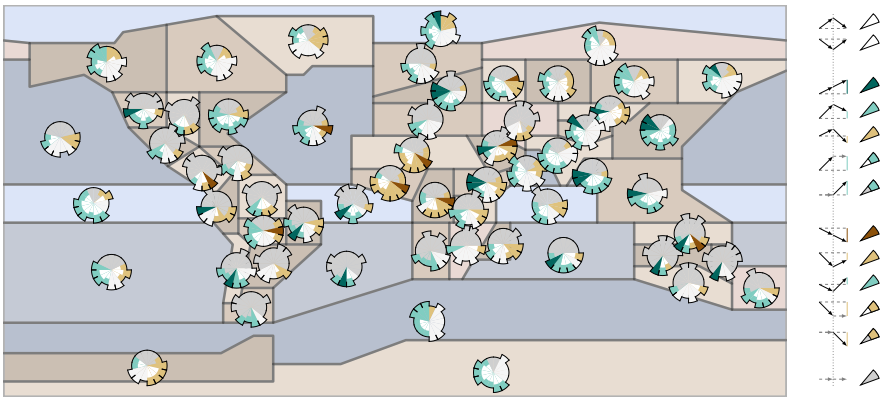

Figure 7. As figure 4 but for annual precipitation.

Precipitation does not follow GMST as closely as surface air temperatures as precipitation changes are dominated by circulation changes. Therefore, the evolution of precipitation throughout the overshoot is more complex and there is a wider variety of possible combinations of trends before and after the overshoot. Overall, there are only few regions where changes in the warming period of the overshoot are robustly reversed afterwards (see fig. 7). In many regions, the period after and before peak warming are to short to identify robust changes and more simulations would be required to analyze the evolution of precipitation changes around the overshoot. In figure 7 this is reflected by many gray circle segments in regional pie-charts.

For the Sahara (SAH), West Africa (WAF) and central Africa (CAF) drying is projected as a result of the overshoot. In the case of West Africa an increase in precipitation is projected by most models in the period where the global climate is warming. The drying in the period when the climate is cooling is however considerably stronger leading to drier conditions after the overshoot at the same GMST level (see fig. 8a-c). GISS-E2-1-G projects a decrease in precipitation before as well as after peak warming leading to 3% less annual precipitation after the overshoot. This finding is in line with Samset et al. [20] who shows that an increase in greenhouse gas concentrations first leads to more precipitation over western Africa but to a drying in the long-term and a similar effect has also been found in a longer overshoot experiment with the community earth system model [10].

Over East Asia (EAS), South Asia (SAS) and South-East Asia (SEA) models consistently project an increase in precipitation as a result of the overshoot. For East Asia (EAS), the majority of models project a continued increase in precipitation irrespective of the reduction in GMST. The consistent increase in precipitation in the period approaching net-zero CO2 emissions is likely a result of a decrease in aerosol concentrations over eastern Asia [21, 22, 23]. The differences in annual precipitation between after and before peak warming at the same GMST are therefore expected.

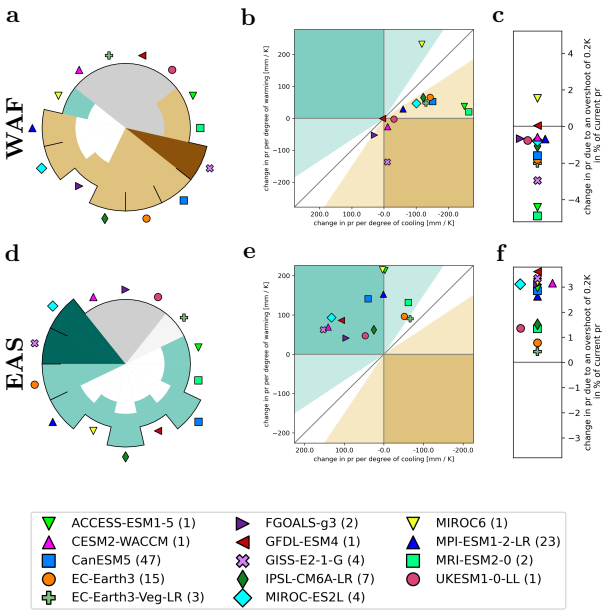

Figure 8. As figure 6 but for annual precipitation over West Africa (WAF a-c) and East Asia (EAS d-f).

3.3. Climate extremes indices

As for surface air temperature, changes in temperatures of the hottest days (TXx) and the coldest nights (TNn) are projected to be reversed in many regions (see fig. 9 and 10). In regions such as the Southern Ocean or the Arctic Ocean, some models project an increase in TXx and TNn that is only partially reversed after peak warming. Also in Northern Europe over land, particularly TNn will be warmer than before the overshoot. Over most other land regions, the coldest nights are projected to be cooler after the overshoot as compared to before peak warming at the same GMST level. This features appears to be quite robust across models over the Sahara (SAH), the Arabic peninsula (ARP) and western central Asia (WCA).

Overall, the projections show a tendency towards warmer hot extremes and cooler cold extremes as a result of the overshoot. For instance, over most African regions the increase in TXx is not fully reversed after peak warming while the increase in TNn is overcompensated in the period after peak warming.

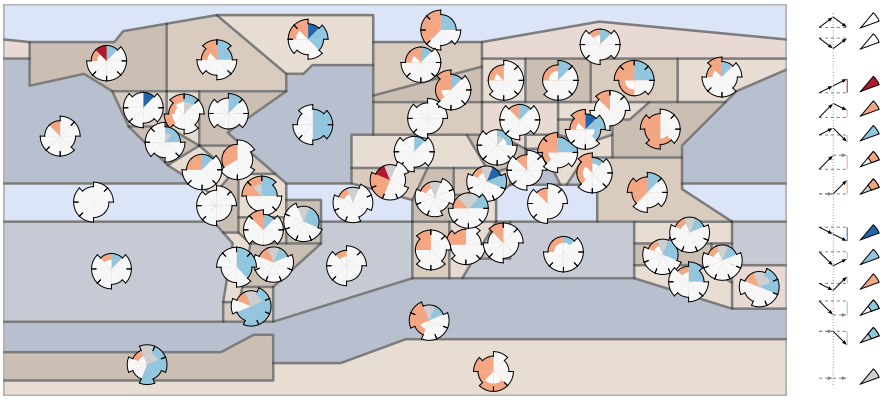

Figure 9. As figure 4 but for TXx

Intense precipitation increases around the globe as climate is warming. However, climate model projections suggest, that these changes are not fully reversed when the climate is cooling in an overshoot scenario. In many cases, changes in RX1day after peak warming cannot be differentiated from natural variability while a robust increase in RX1day is projected for the period before peak warming. These changes are particularly consistent in East Asia (EAS) and South Asia (SAS) where also an increase in annual precipitation is projected. As for precipitation (see section 3.2) some of these asymmetries in the evolution of extreme precipitation throughout the overshoot might be a result of changes in aerosol concentrations.

Regions for which a drying effect of the overshoot is projected are likely to also experience a reduction in intense precipitation (see WAF, CAF).

GFDL-ESM4 and MIROC-ES2L project a continued increase in extreme precipitation for many regions around the globe (see figure 17) and GFDL-ESM4 also projects a continued decrease in extreme precipitation for Australia. The extreme changes in these models can not be explained by changes in regional aerosol emissions

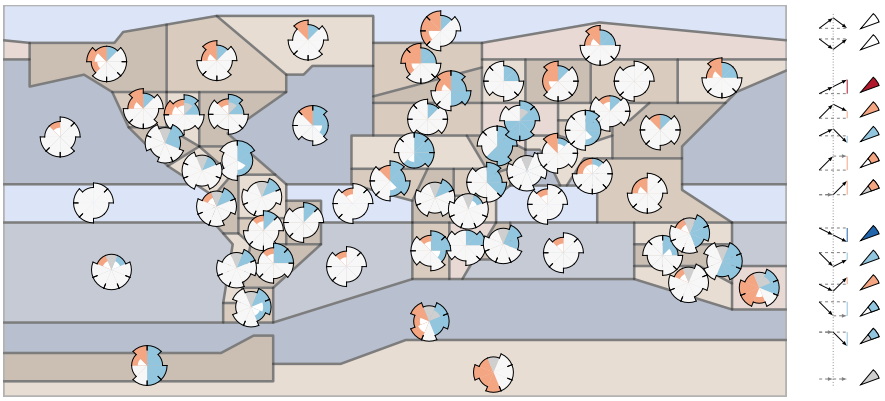

Figure 10. As figure 4 but for TNn

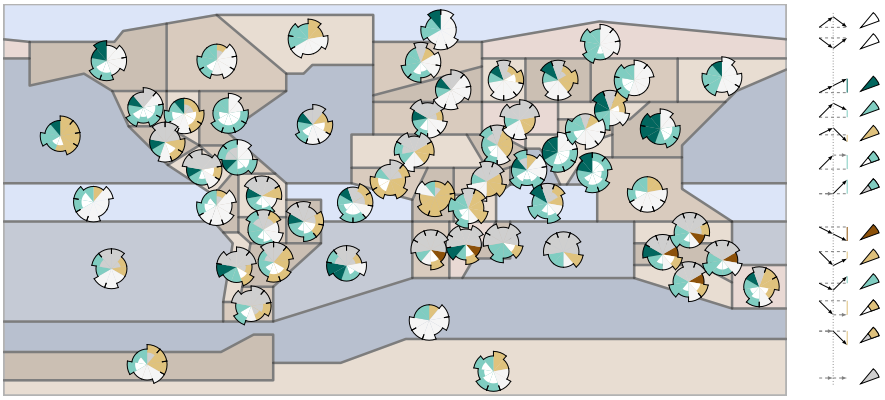

Figure 11. As figure 4 but for RX1day

only. Changes in atmospheric circulation as a response to changes in SST patterns might explain these changes. Note that the sensitivity to changes in precipitation and extreme precipitation patterns varies strongly across models (compare 14 and 17).

4. Discussion and conclusions

Climate projections of overshoot scenarios show that changes in regional climate signals are not reversed in the decades after peak warming when a reduction in CO2 concentrations decreases global mean surface air temperature (GMST). The evolution of regional climate signals throughout the overshoot is complex and in some regions highly non-linear such that the dependence of regional temperature and precipitation on GMST changes considerably around peak warming.

Our analysis of the SSP1-19 and the SSP5-34-OS scenario shows that different regional temperature patterns would emerge for the period after peak warming. As a result, at the same GMST level after peak warming, some regions are projected to be considerably warmer or cooler after peak warming when compared to a period with similar GMST levels before peak warming.

For the Southern Ocean and the South Atlantic models project that the warming in the period before peak warming is not or only partially reversed afterwards. For the North Atlantic the opposite behavior is projected. These changes can be explained by the pattern effect for which the slow response to an increase in CO2 concentrations shows a strong warming signal in the Southern Ocean [12]. Over land, most models project that annual mean surface air temperatures follow closely GMST. There are however also land regions where models consistently project cooler (northern Asia) or warmer (southern Asia) temperatures.

The asymmetries in the evolution of regional climate signals throughout the overshoot is more pronounced for precipitation than for temperatures and there are only few regions for which models project that the changes before peak warming would be robustly reversed after peak warming. There are however also a number of region-model combinations where the analyzed periods before and after peak warming are too short to robustly identify changes in precipitation.

For western Africa, climate models consistently project that the drying after peak warming overcompensates the increase in precipitation before peak warming with some models even projecting a continued drying in this region. These changes might be related to the hysteresis in the inter-tropical convergence zone as reported by [10].

For East Asia, models consistently project an increase in precipitation in the period before peak warming that is followed by continued increase or a weak decrease in precipitation afterwards. As a result, we expect higher precipitation and particularly more intense precipitation in the period after peak warming as compared to before peak warming. These changes can be explained by the reductions in aerosol emissions in that region that lead to a considerable increase in precipitation in the period approaching net-zero emissions where aerosol emissions are reduced [21, 22, 23, 24].

Changes in aerosol concentrations are affecting precipitation (and temperatures) globally by altering regional radiation balances and thereby also affecting circulation patterns [25, 26, 27]. In an overshoot scenario, aerosol emissions are strongly reduced until net-zero CO2 emissions are reached without major changes in aerosol emissions

thereafter. As a result changes related to aerosol concentrations before peak warming are without a counterpart in the period after peak warming leading to asymmetric behaviors in regional climate signals [28].

Changes in seasonal climate signals as well as changes in climate extremes indices are more pronounced than annual mean temperature or annual precipitation. Our analysis suggests, that the increase in intense precipitation will not be reversed in the decades following peak warming. Cold extremes are projected to be more colder in the period after the overshoot over most land regions except high-latitude regions, where differences in snow/ice coverage may lead to warmer TNn after overshoot. Hot extremes are projected to be hotter over Africa and eastern Asia, while in the Arctic diverse behaviors are projected. Further research on dynamical changes in atmospheric and oceanic circulation would be required to get a better estimate on how weather extreme events might change in a cooling climate.

The evolution of regional climate signals throughout the overshoot results from the combination of different dynamic effects that potentially interact in complex ways. The superposition of the instantaneous response to the reduction in greenhouse gas concentrations after peak warming with the long-term and slow responses to the emissions in the decades before peak warming [13, 12] as well as the above mentioned effects of aerosol emissions before peak warming lead to a shift in regional sea surface temperature patterns. These changes have far reaching implications for atmospheric circulation, moisture transport and thereby regional climate signals [29, 30, 31].

On top of these changes, local feedback mechanisms and changes in ecosystems during the overshoot might have long-term effects for local and regional climatic conditions. The representation of local effects such as changes in vegetation [32] or permafrost [33] are still a challenge for Earth System models. We therefore expect that Earth System models underestimate the impacts of an overshoot on regional climate. For example, the projected warming for northeastern North America might cause further local impacts on permafrost.

Climate model projection suggest that many impacts of an overshoot would not be reversed and that especially impacts related to the water cycle such as water scarcity or intense precipitation mainly scale with the intensity of the overshoot and not with the GMST levels afterwards. The same could apply for temperature changes in hotspot regions and other seasonal impacts. In combination with global or regional tipping points [34, 35] and the uncertainties related to the effectiveness of methods to reduce CO2 concentrations in the atmosphere our analysis adds to the reasons that irreversible risks may be inferred by overshoots.

5. References

[1] Haustein K, Allen M R, Forster P M, Otto F E L, Mitchell D M, Matthews H D and Frame D J 2017 *Scientific Reports* **7** 15417 ISSN 2045-2322

[2] IPCC 2022 Summary for policymakers *Climate Change 2022: Mitigation of Climate Change. Contribution of Working Group III to the Sixth Assessment Report of the Intergovernmental Panel on Climate Change* ed Shukla P, Skea J, Slade R, Khourdajie A A, van Diemen R, McCollum D, Pathak M, Some S, Vyas P, Fradera R, Belkacemi M, Hasija A, Lisboa G, Luz S and Malley J (Cambridge, UK and New York, NY, USA: Cambridge University Press)

[3] Schleussner C F, Rogelj J, Schaeffer M, Lissner T, Licker R, Fischer E M, Knutti R, Levermann A, Frieler K and Hare W 2016 *Nature Climate Change* **6** 827–835 ISSN 1758-6798

[4] Mengel M, Nauels A, Rogelj J and Schleussner C F 2018 *Nature Communications* **9** 601 ISSN 2041-1723

[5] Lee H, Calvin K, Dasgupta D, Krinner G, Mukherji A, Thorne P, Trisos C, Romero J, Aldunce P, Barrett K, Blanco G, Cheung W W L, Connors S L, Denton F, Diongue-Niang A, Dodman D, Garschagen M, Geden O, Hayward B, Jones C, Jotzo F, Krug T, Lasco R, Lee J Y, Masson-Delmotte V, Meinshausen M, Mintenbeck K, Mokssit A, Otto F E L, Pathak M, Pirani A, Poloczanska E, Pörtner H O, Revi A, Roberts D C, Roy J, Ruane A C, Skea J, Shukla P R, Slade R, Slangen A, Sokona Y, Sörensson A A, Tignor M, van Vuuren D, Wei Y M, Winkler H, Zhai P and Zommers Z 2023 Synthesis report of the IPCC sixth assessment report (AR6): Summary for policymakers

[6] Ranasinghe R, Ruane A, Vautard R, Arnell N, Coppola E, Cruz F, Dessai S, Islam A, Rahimi M, Ruiz Carrascal D, Sillmann J, Sylla M, Tebaldi C, Wang W and Zaaboul R 2021 Climate change information for regional impact and for risk assessment *Climate Change 2021: The Physical Science Basis. Contribution of Working Group I to the Sixth Assessment Report of the Intergovernmental Panel on Climate Change* ed Masson-Delmotte V, Zhai P, Pirani A, Connors S, Péan C, Berger S, Caud N, Chen Y, Goldfarb L, Gomis M, Huang M, Leitzell K, Lonnoy E, Matthews J, Maycock T, Waterfield T, Yelekçi O, Yu R and Zhou B (Cambridge, United Kingdom and New York, NY, USA: Cambridge University Press) pp 1767–1926

[7] Tokarska K B, Zickfeld K and Rogelj J 2019 *Earth's Future* **7** 1283–1295 ISSN 2328-4277

[8] Boucher O, Halloran P R, Burke E J, Doutriaux-Boucher M, Jones C D, Lowe J, Ringer M A, Robertson E and Wu P 2012 *Environmental Research Letters* **7** 024013 ISSN 1748-9326

[9] Melnikova I, Boucher O, Cadule P, Ciais P, Gasser T, Quilcaille Y, Shiogama H, Tachiiri K, Yokohata T and Tanaka K 2021 *Earth's Future* **9** e2020EF001967 ISSN 2328-4277

[10] Kug J S, Oh J H, An S I, Yeh S W, Min S K, Son S W, Kam J, Ham Y G and Shin J 2021 *Nature Climate Change* 1–7 ISSN 1758-6798

[11] Held I M, Winton M, Takahashi K, Delworth T, Zeng F and Vallis G K 2010 *Journal of Climate* **23** 2418–2427 ISSN 1520-0442, 0894-8755

[12] Ceppi P, Zappa G, Shepherd T G and Gregory J M 2018 *Journal of Climate* **31** 1091–1105 ISSN 0894-8755, 1520-0442

[13] Dong Y, Armour K C, Zelinka M D, Proistosescu C, Battisti D S, Zhou C and Andrews T 2020 *Journal of Climate* **33** 7755–7775 ISSN 0894-8755, 1520-0442

[14] Manabe S, Stouffer R J, Spelman M J and Bryan K 1991 *Journal of Climate* **4** 785–818 ISSN 0894-8755, 1520-0442

[15] King A D, Borowiak A R, Brown J R, Frame D J, Harrington L J, Min S K, Pendergrass A, Rugenstein M, Sniderman J M K and Stone D A 2021 *Earth's Future* **9** e2021EF002274 ISSN 2328-4277

[16] Seneviratne S I, Rogelj J, Séférian R, Wartenburger R, Allen M R, Cain M, Millar R J, Ebi K L, Ellis N, Hoegh-Guldberg O, Payne A J, Schleussner C F, Tschakert P and Warren R F 2018 *Nature* **558** 41–49 ISSN 1476-4687

[17] Eyring V, Bony S, Meehl G A, Senior C A, Stevens B, Stouffer R J and Taylor K E 2016

Geoscientific Model Development **9** 1937–1958 ISSN 1991-959X

[18] O'Neill B C, Tebaldi C, van Vuuren D P, Eyring V, Friedlingstein P, Hurtt G, Knutti R, Kriegler E, Lamarque J F, Lowe J, Meehl G A, Moss R, Riahi K and Sanderson B M 2016 *Geoscientific Model Development* **9** 3461–3482 ISSN 1991-959X

[19] Schleussner C F, Runge J, Lehmann J and Levermann A 2014 *Earth System Dynamics* **5** 103–115 ISSN 2190-4979

[20] Samset B H, Myhre G, Forster P M, Hodnebrog Ø, Andrews T, Faluvegi G, Fläschner D, Kasoar M, Kharin V, Kirkevåg A, Lamarque J F, Olivié D, Richardson T, Shindell D, Shine K P, Takemura T and Voulgarakis A 2016 *Geophysical Research Letters* **43** 2782–2791 ISSN 1944-8007

[21] Liu L, Shawki D, Voulgarakis A, Kasoar M, Samset B H, Myhre G, Forster P M, Hodnebrog Ø, Sillmann J, Aalbergsjø S G, Boucher O, Faluvegi G, Iversen T, Kirkevåg A, Lamarque J F, Olivié D, Richardson T, Shindell D and Takemura T 2018 *Journal of Climate* **31** 4429–4447 ISSN 0894-8755, 1520-0442

[22] Samset B H, Sand M, Smith C J, Bauer S E, Forster P M, Fuglestvedt J S, Osprey S and Schleussner C F 2018 *Geophysical Research Letters* **45** 1020–1029 ISSN 0094-8276, 1944-8007

[23] Sillmann J, Stjern C W, Myhre G, Samset B H, Hodnebrog Ø, Andrews T, Boucher O, Faluvegi G, Forster P, Kasoar M R, Kharin V V, Kirkevåg A, Lamarque J F, Olivié D J L, Richardson T B, Shindell D, Takemura T, Voulgarakis A and Zwiers F W 2019 *npj Climate and Atmospheric Science* **2** 1–7 ISSN 2397-3722

[24] Wilcox L J, Liu Z, Samset B H, Hawkins E, Lund M T, Nordling K, Undorf S, Bollasina M, Ekman A M L, Krishnan S, Merikanto J and Turner A G 2020 *Atmospheric Chemistry and Physics* **20** 11955–11977 ISSN 1680-7316

[25] Hwang Y T, Frierson D M W and Kang S M 2013 *Geophysical Research Letters* **40** 2845–2850 ISSN 1944-8007

[26] Haywood J M, Jones A, Bellouin N and Stephenson D 2013 *Nature Climate Change* **3** 660–665 ISSN 1758-6798

[27] Samset B H, Sand M, Smith C J, Bauer S E, Forster P M, Fuglestvedt J S, Osprey S and Schleussner C F 2018 *Geophysical Research Letters* **45** 1020–1029 ISSN 1944-8007

[28] Persad G G, Samset B H and Wilcox L J 2022 *Nature* **611** 662–664

[29] He J and Soden B J 2017 *Nature Climate Change* **7** 53–57 ISSN 1758-678X, 1758-6798

[30] Zappa G, Ceppi P and Shepherd T G 2020 *Proceedings of the National Academy of Sciences* **117** 4539–4545 ISSN 0027-8424, 1091-6490

[31] Hou H, Qu X and Huang G 2021 *Earth's Future* **9** ISSN 2328-4277, 2328-4277

[32] Song X, Wang D Y, Li F and Zeng X D 2021 *Advances in Climate Change Research* **12** 584–595 ISSN 1674-9278

[33] Burke E J, Zhang Y and Krinner G 2020 *The Cryosphere* **14** 3155–3174 ISSN 1994-0416

[34] Wunderling N, Winkelmann R, Rockström J, Loriani S, Armstrong McKay D I, Ritchie P D L, Sakschewski B and Donges J F 2023 *Nature Climate Change* **13** 75–82 ISSN 1758-6798

[35] Kloenne U, Nauels A, Pearson P, DeConto R M, Findlay H S, Hugelius G, Robinson A, Rogelj J, Schuur E A G, Stroeve J and Schleussner C F 2023 *Nature Climate Change* **13** 9–11 ISSN 1758-6798

6. Conflict of interests

The authors declare no conflict of interests.

7. Data availability statement

The analyzed CMIP6 simulations are freely available under `https://esgf-node.llnl.gov/search/cmip6/`.

8. Funding acknoledgements

All authors acknowledge funding from the European Union's Horizon 2020 research and innovation programmes under grant agreement No 101003687 (PROVIDE).

9. Appendix

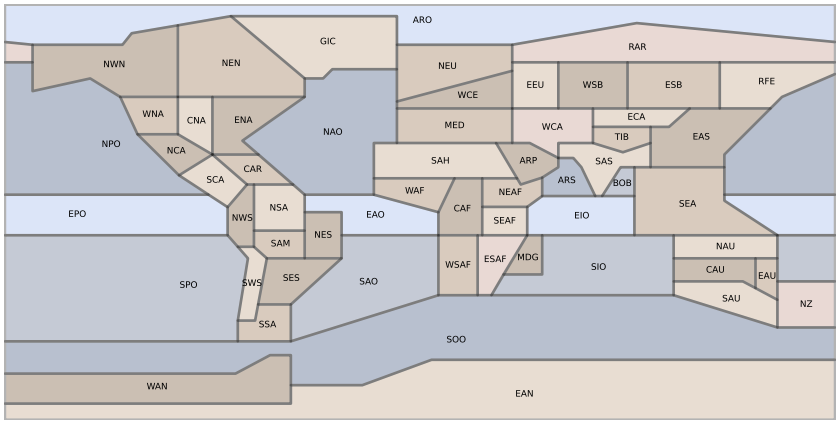

Figure 12. Regions as used in the 6th assessment report of the Intergovernemental Panel on Climate Change.

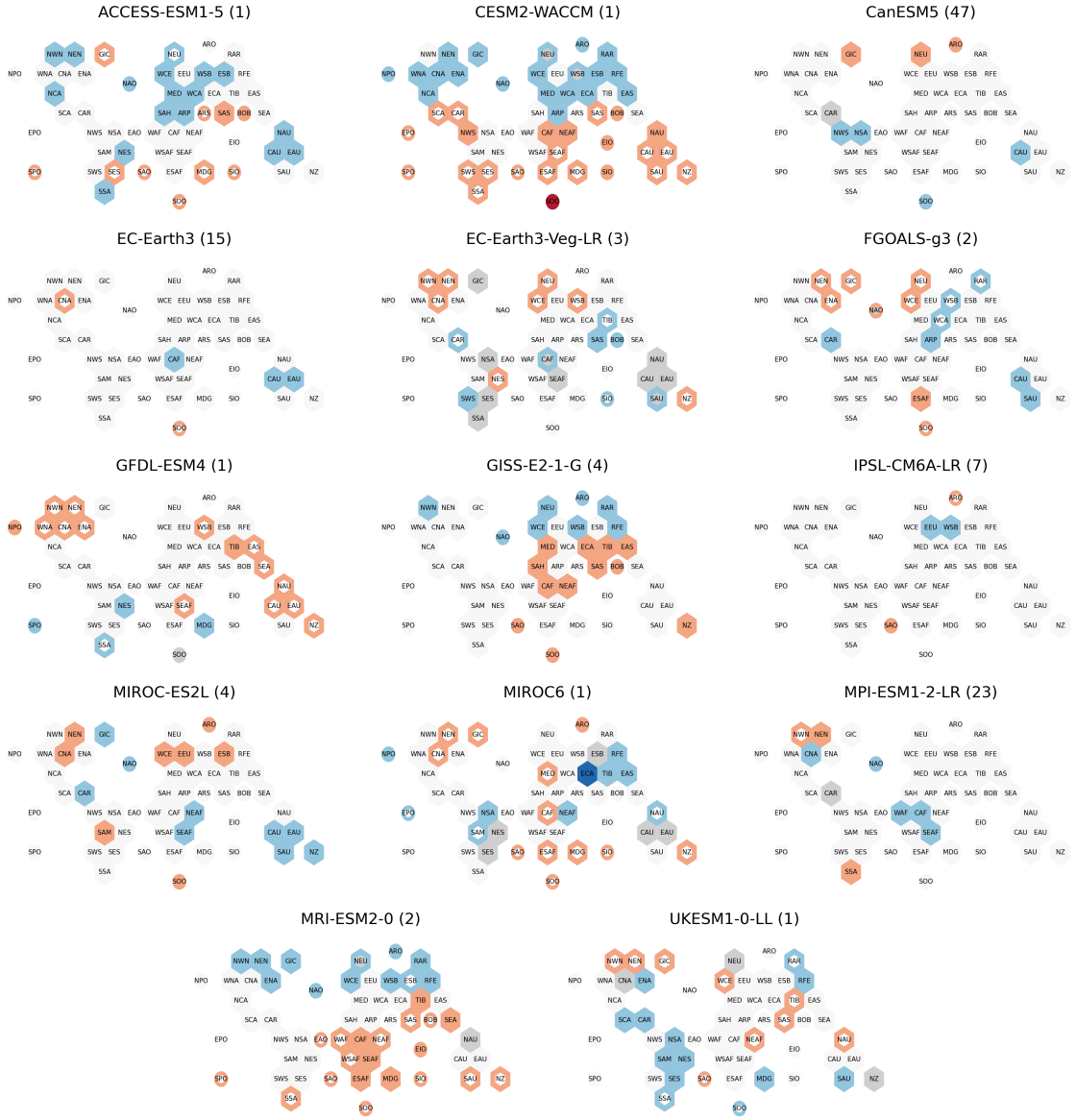

Figure 13. Changes in annual surface air temperature around peak warming. The coloring of land-region hexagon and ocean-region circles follows the logic of table 2. Red (blue) colors indicate that the overshoot leads to warmer (cooler) local conditions. If the inner part of a region is white (gray) it means that there is no robust trend after (before) peak warming.

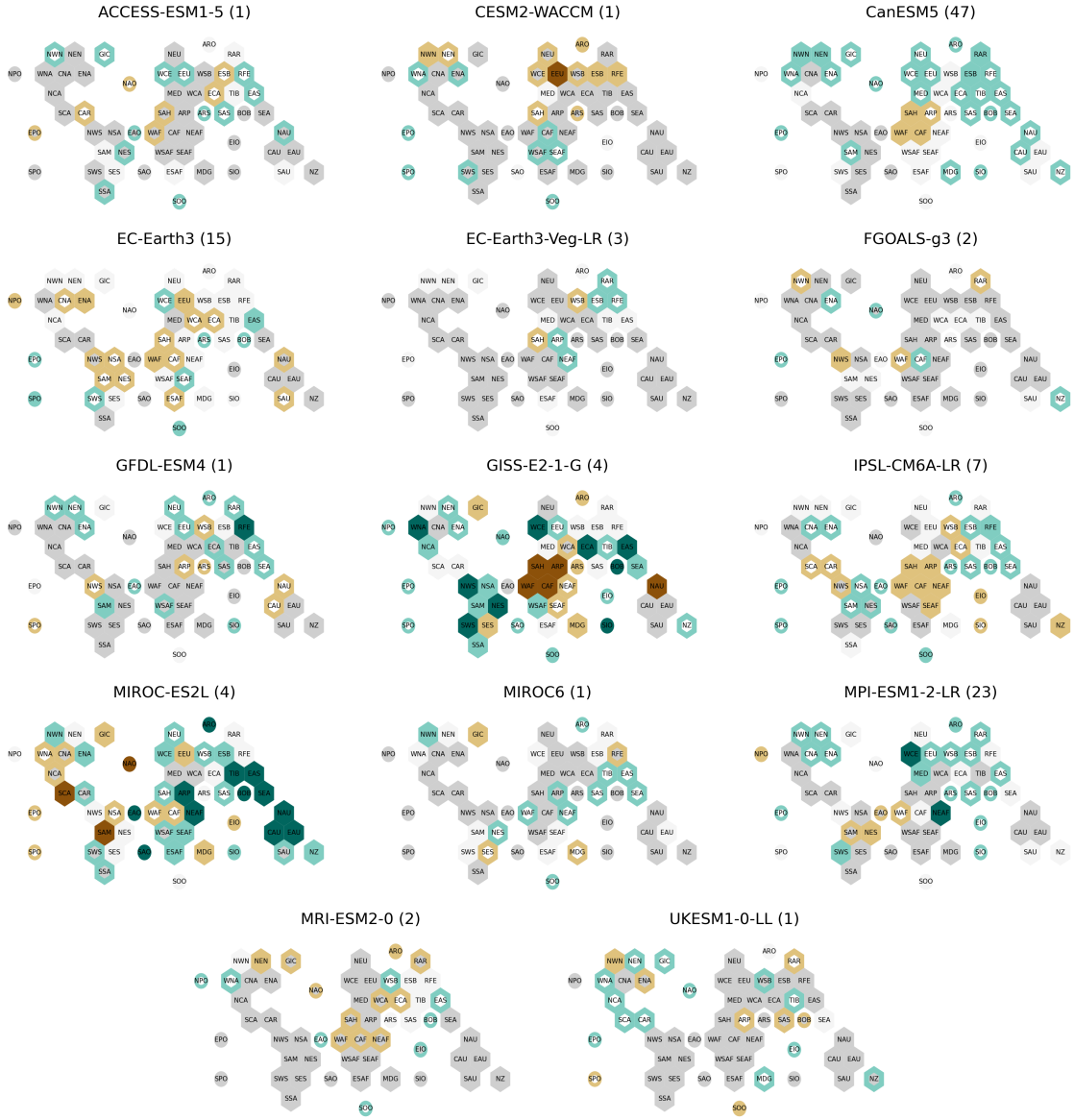

Figure 14. As figure 13 but for annual precipitation.

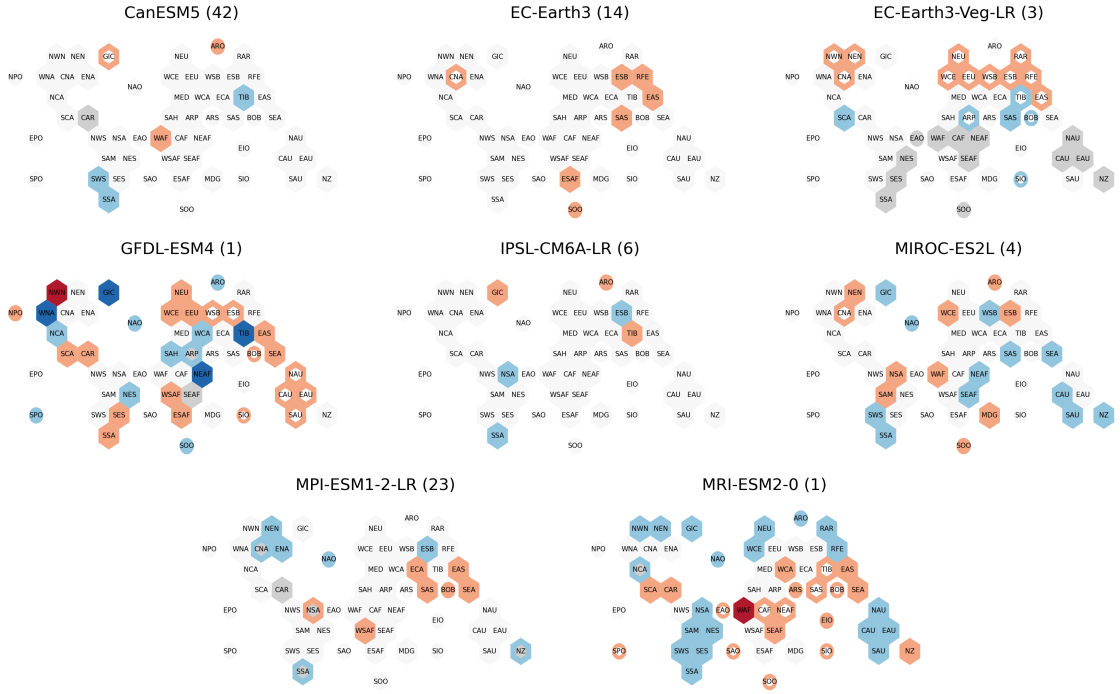

Figure 15. As figure 13 but for TXx.

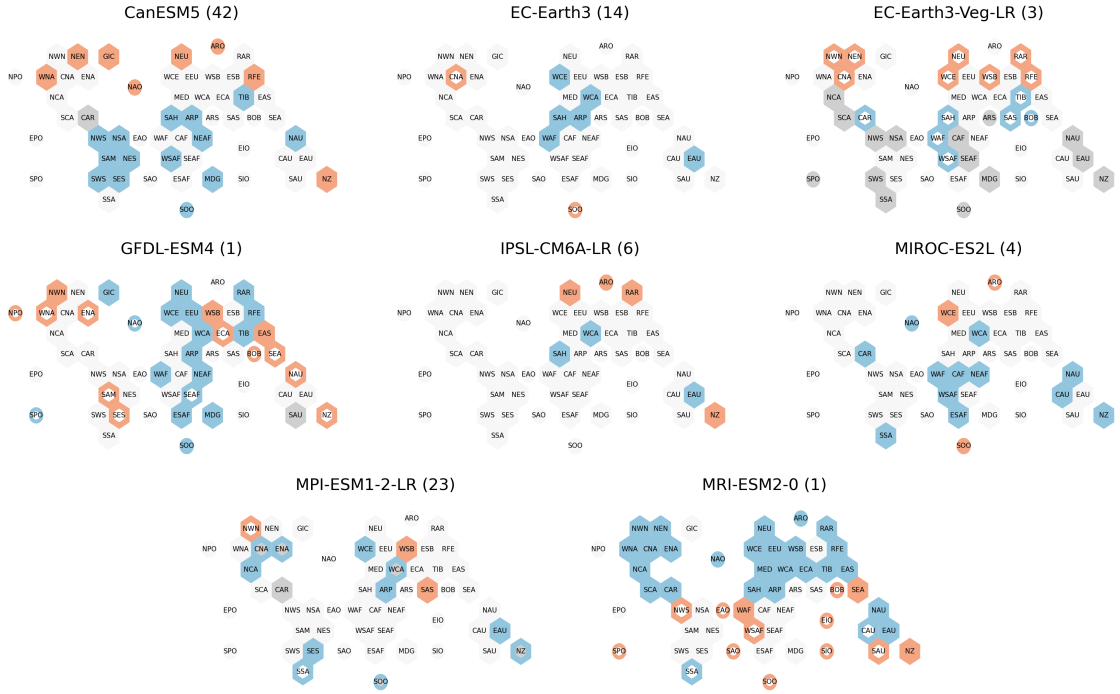

Figure 16. As figure 13 but for Tnn.

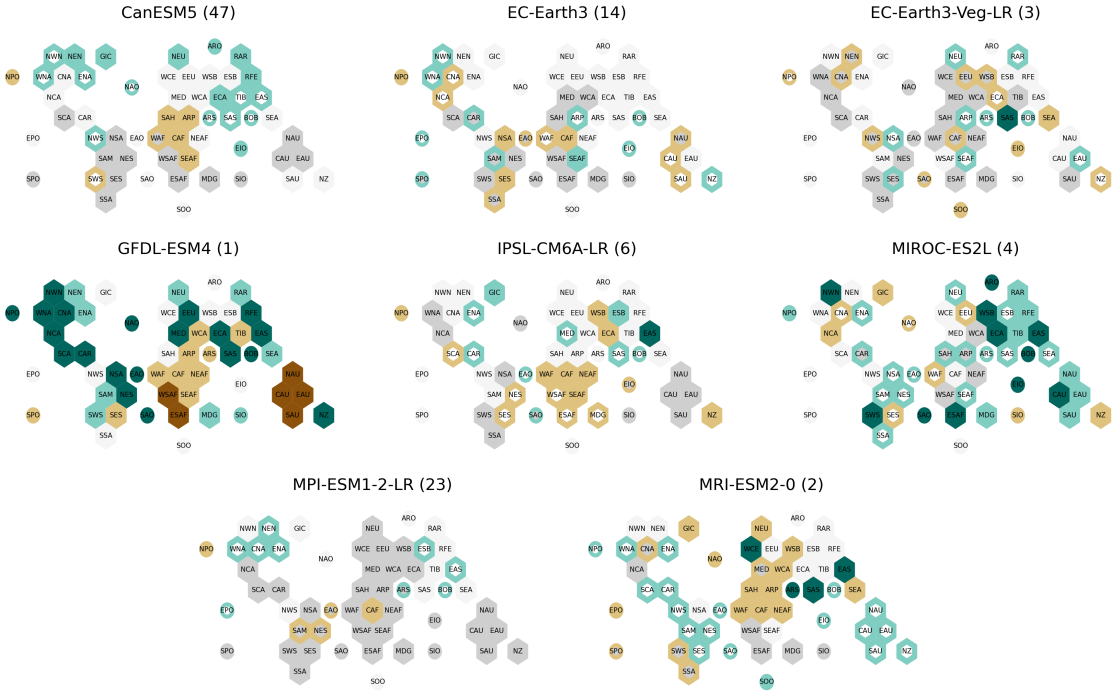

Figure 17. As figure 13 but for Rx1day.